IEEE Photonics Journal
An IEEE Photonics Society Publication

Open Access

Dynamics of 1550-nm VCSELs With Positive Optoelectronic Feedback: Theory and Experiments

Volume 6, Number 6, December 2014

Yi-Yuan Xie
Hong-Jun Che
Wei-Lun Zhao
Ye-Xiong Huang
Wei-Hua Xu
Xin Li
Qian Kan
Jia-Chao Li

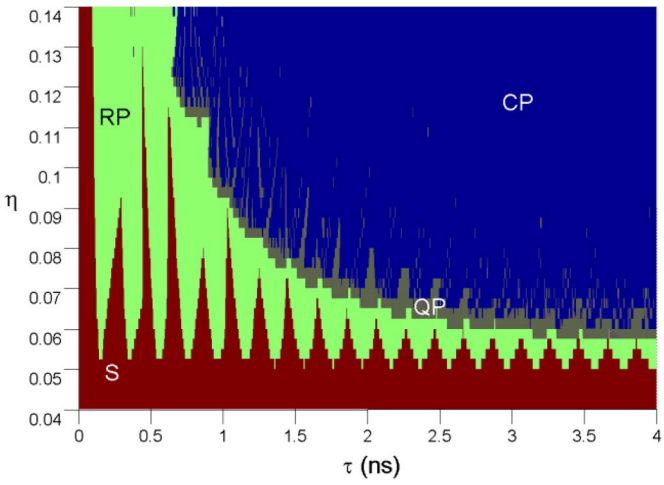

DOI: 10.1109/JPHOT.2014.2368775
1943-0655 © 2014 IEEE

IEEE photonics SOCIETY

IEEE

Dynamics of 1550-nm VCSELs With Positive Optoelectronic Feedback: Theory and Experiments

Yi-Yuan Xie, Hong-Jun Che, Wei-Lun Zhao, Ye-Xiong Huang, Wei-Hua Xu, Xin Li, Qian Kan, and Jia-Chao Li

School of Electronic and Information Engineering, Southwest University, Chongqing 400715, China

DOI: 10.1109/JPHOT.2014.2368775
1943-0655 © 2014 IEEE. Translations and content mining are permitted for academic research only. Personal use is also permitted, but republication/redistribution requires IEEE permission. See http://www.ieee.org/publications_standards/publications/rights/index.html for more information.

Manuscript received September 10, 2014; revised October 27, 2014; accepted October 29, 2014. Date of publication November 7, 2014; date of current version December 2, 2014. This work was supported in part by the National Natural Science Foundation of China under Grant 61205088, by the Natural Science Foundation of Chongqing Municipal under Grant 2011BB2009, and by the Fundamental Research Funds for the Central Universities under Grant XDJK2014A017. Corresponding author: Y. Y. Xie (e-mail: yyxie@swu.edu.cn).

Abstract: Nonlinear dynamics of a 1550-nm vertical-cavity surface-emitting laser with positive optoelectronic feedback are studied both numerically and experimentally. A mapping of dynamical states is presented in the parameter space of feedback delay time and feedback strength, where different states are identified and shown. A bifurcation diagram of the extrema of output peak series versus the feedback delay time is plotted. Various nonlinear dynamical behaviors, including regular pulsing, quasi-periodic pulsing, and chaotic pulsing, have been numerically and experimentally observed. Both numerical simulation and experimental observation indicate that the laser enters a chaotic pulsing state at certain delay times of the feedback loop through a quasi-periodic route.

Index Terms: 1550-nm vertical-cavity surface-emitting laser (1550-nm VCSEL), nonlinear dynamics, positive optoelectronic feedback (POEF).

1. Introduction

Vertical-cavity surface emitting lasers (VCSELs) are important candidates for applications in optical communication, big data centers, optical interconnects inter/intra chips, and other relevant fields because of their inherent advantages over conventional edge-emitting semiconductor lasers (EELs). These advantages include low threshold current, single longitudinal-mode operation, excellent circular output beam with narrow divergence, low cost, easy large-scale integration into 2-D arrays, etc. [1]–[5].

Because VCSELs play the important roles in many fields, study on the nonlinear dynamics of VCSELs is particularly important and has been widely studied. Previous theoretical and experimental research studies have demonstrated that VCSELs exhibit a wide range of nonlinear dynamics under external perturbations including optical injection, optical feedback or optoelectronic feedback (OEF) [6]–[27]. For OEF, the laser output is converted into electric current through a photodetector and fed back to the laser. Different phenomena of VCSELs subject to optical injection or optical feedback have been studied and reported in recent years. These phenomena include polarization switching (PS) and bistability [6]–[13]; injection locking [14], and [15]; nonlinear dynamics, such as regular pulsing (RP), quasiperiodic pulsing (QP), chaos [16]–[27], etc.

In comparison with optical injection and optical feedback, OEF is more flexible and reliable because of its convenience to be electronically controlled and its insensitivity to optical phase variations [28]–[30]. For OEF through the injection current, there are two categories, one is negative optoelectronic feedback (NOEF) and the other is positive optoelectronic feedback (POEF). In NOEF, the feedback current is deducted from the bias injection current, and in POEF, the feedback current is added to the bias injection current. Several research studies on the polarization dynamics of VCSELs with NOEF [31] and POEF [32] have been investigated, and various dynamical states such as period-1 (P1), two-frequency quasiperiodic (Q2), three-frequency quasiperiodic (Q3) and chaos are also observed, but most of these studies focus on the short-wavelength VCSELs (~800–1000 nm). Recently, long-wavelength VCSELs emitting at the important telecom wavelength of 1550 nm have attracted increasing interest because of their important applications in optical networks [11], [12]. However, studies on the nonlinear dynamics of 1550 nm VCSELs subject OEF are relatively inadequate. Thus, we recently pay our attention to it and we have experimentally studied the nonlinear dynamics of 1550 nm with POEF by varying the feedback strength [33]. The rich variety of the nonlinear dynamics of 1550 nm VCSELs subject to OEF offers exciting prospects for the practical use of these devices in novel applications in optical networks.

To further research on the dynamics of 1550 nm VCSELs with POEF, in this paper, we report, to the best of our knowledge for the first time, the nonlinear dynamics of a 1550 nm VCSEL with POEF through varying the feedback delay time is studied numerically and experimentally. In the numerically analysis, a mapping of the dynamic states is plotted in the parameter space of the feedback delay time and the feedback strength. Meanwhile, a bifurcation diagram of the extrema of output peak series versus the feedback delay time is plotted. Various dynamical states, which are determined by combining the output time series, power spectra and phase portraits, have been observed numerically and experimentally. Although, theoretical and experimental results have some small discrepancies, they show good agreement because the basic dynamic states, including the RP, QP, and CP states and the quasiperiodic route to chaos, are similar.

2. Numerical Analysis

The rate equation model for VCSEL with POEF is based on the San Miguel, Feng, and Moloney model also called spin-flip model (SFM) [34], [35]. It includes the light polarization degree of freedom for the free-running VCSEL as a result of a four-level model that takes into account the lasing transitions between the spin sublevels of the conduction and valence bands of a quantum well semiconductor. The SFM model can be extended to account for the optoelectronic feedback by introducing an additional delayed term in the current [31], [32]. The rate equations for VCSEL with POEF can be described by

$$\frac{\mathrm{d}E_x}{dt} = \kappa(1+i\alpha)\left[(N-1)E_x + inE_y\right] - (\gamma_a + i\gamma_p)E_x + \sqrt{\beta_{sp}}\xi_x \tag{1}$$

$$\frac{dE_y}{dt} = \kappa(1+i\alpha)\left[(N-1)E_y - inE_x\right] + (\gamma_a + i\gamma_p)E_y + \sqrt{\beta_{sp}}\xi_y \tag{2}$$

$$\frac{dN}{dt} = -\gamma_e N(1+P) + \gamma_e\mu\left[1+\eta\frac{P(t-\tau)}{P_0}\right] - i\gamma_e n\left(E_yE_x^* - E_xE_y^*\right) \tag{3}$$

$$\frac{dn}{dt} = -\gamma_s n - \gamma_e nP - i\gamma_e N\left(E_yE_x^* - E_xE_y^*\right) \tag{4}$$

where subscripts x and y represent x and y linear polarized modes, respectively. E is the slowly varied complex amplitude of the field, N is the total carrier inversion between the conduction and valence bands, n accounts for the difference between carrier inversions for the spin-up and spin-down radiation channels. The internal VCSEL parameters are as follows: k is the cavity delay rate, α is the linewidth enhancement factor, γ_e is the decay rate of total carrier population, γ_a is the gain anisotropy rate, γ_p is the linear birefringence rate, and γ_s is the spin relaxation rate. τ is the feedback delay time, μ is the normalized injection current, η is the feedback index

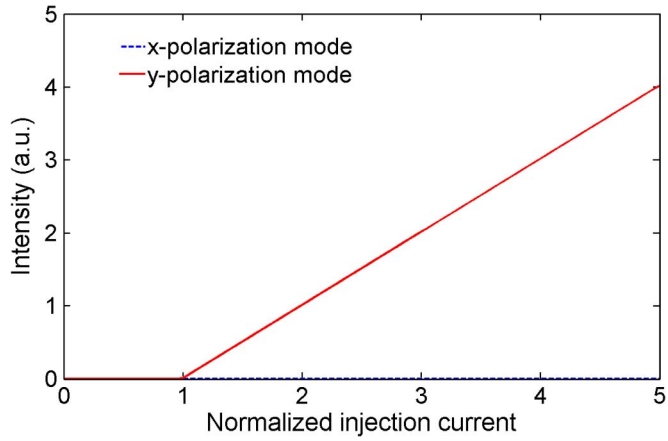

Fig. 1. Numerically calculated P–I curve of a free-running 1550 nm VCSEL. Dash line: x-polarization mode; solid line: y-polarization mode.

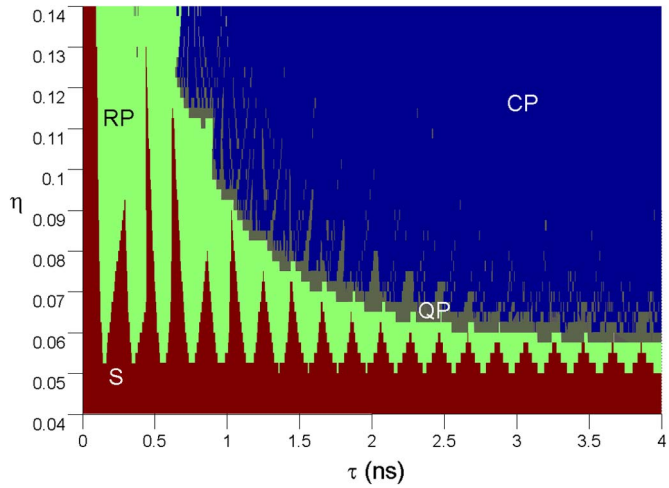

Fig. 2. Calculated mapping of the dynamic states of the 1550 nm VCSEL subject to POEF in the parameter space of (τ, η), where the normalized injection current μ is fixed at 2.5. S: steady states. RP: regular pulsing. QP: quasiperiodic pulsing. CP: chaotic pulsing.

corresponding to the strength of feedback, $P = |E_x|^2 + |E_y|^2$ is the normalized output power, and P_0 is the free-running output power. Finally, the effect of spontaneous emission noise is included by introducing a zero mean Gaussian noise source (as given in [11]). β_{sp} is the spontaneous emission factor $(= 10^{-6})$ [11] and $\xi_{x,y}$ are Gaussian white noises of zero mean value.

Equations (1)–(4) can be numerically solved by adopting the fourth-order Runge–Kutta algorithm, and the 1550 nm VCSEL parameters chosen for the simulation are [11]: $\gamma_e = 1$ ns^{-1}, $\gamma_p = 192.1$ ns^{-1}, $\gamma_a = 1$ ns^{-1}, $\gamma_s = 1000$ ns^{-1}, $k = 300$ ns^{-1}, and $\alpha = 3$. With this parameter choice, the free-running 1550 nm VCSEL emits in the y-polarization mode with a threshold current of $\mu_{th} = 1$ and does not show polarization switching over the injected current range studied here (see Fig. 1).

Fig. 2 shows the calculated mapping of the dynamic states of the 1550 nm VCSEL subject to POEF in the parameter space of (τ, η), where the normalized injection current μ is fixed at 2.5. As can be seen, the dynamics of this POEF system become more complicated as the feedback delay time or the feedback strength increases, where the chaotic pulsing states are observed in the regions of long delay times and large feedback strengths. Clearly, this POEF system enters chaos through a quasiperiodic route following RP, QP, and, finally, CP states.

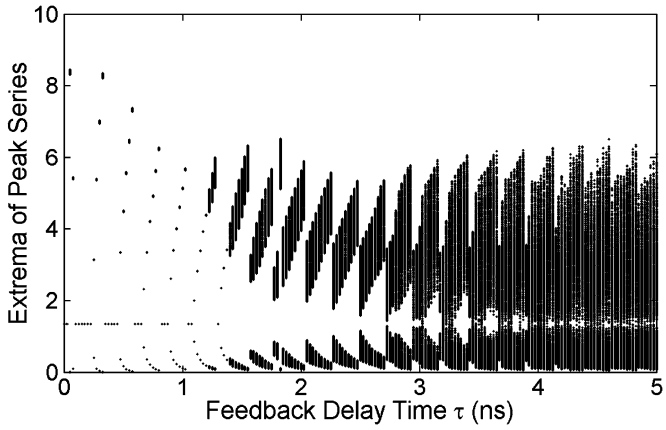

Fig. 3. Calculated bifurcation diagram of the extrema of the peak series versus the feedback delay time for a 1550 nm VCSEL subject to POEF, where the feedback strength and the normalized injection current are fixed at 0.07 and 2.5, respectively.

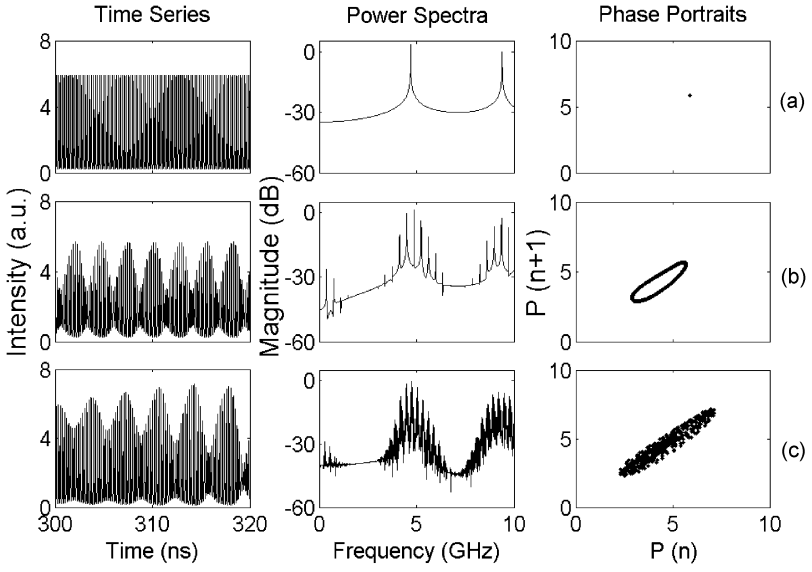

Fig. 4. Numerically calculated time series, power spectra, and phase portraits of different states: (a) RP, (b) QP, and (c) CP states, where the feedback delay times are 1 ns, 2.2 ns, and 3.1 ns, respectively.

In Fig. 3, the extrema of peak series of the POEF system are plotted versus the feedback delay time η, where the feedback strength η and the normalized injection current μ are fixed at 0.07 and 2.5. These extrema of the peak series are obtained by extracting the maxima and minima of the peak series, which make different pulsing states easier to be distinguished. As can be seen in Fig. 3, when the feedback delay time is small, the 1550 nm VCSEL subject to POEF is operated in the RP state. By increasing the feedback delay time, the POEF VCSEL system enters into QP state and finally enters into CP state. In general, the complexity of the dynamics increases for this POEF system with increasing the feedback delay time. To further identify these dynamic states, the time series, the power spectra, and the phase portraits need to be investigated.

Fig. 4(a)–(c) displays the simulation results for different feedback delay time τ, where the time series, the power spectra and the phase portraits of the 1550 nm VCSEL corresponding to the different nonlinear regions are plotted. The optoelectronic feedback strength and the normalized

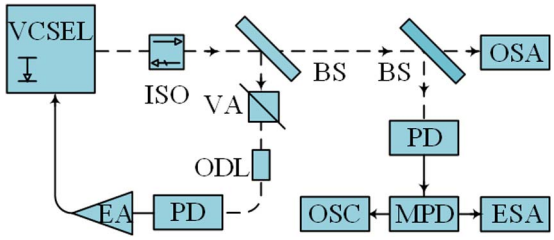

Fig. 5. Schematic diagram of the experimental setup. Dashed line: optical path; solid line: electronic path; ISO: isolator; BS: beam splitter; VA: variable attenuator; ODL: optical delay line; PD: photoelectronic detector; EA: electronic amplifier; OSA: optical spectrum analyzer; MPD: microwave power divider; OSC: digital oscilloscope; ESA: radio-frequency spectrum analyzer.

injection current are fixed at $\eta = 0.07$ and $\mu = 2.5$ while τ is changed. For $\tau = 1$ ns, as shown in Fig. 4(a), the system is in a RP state, where the time series shows a sequence of regular pulses with a constant pulsing intensity and interval. The corresponding power spectrum has a dominant peak at $f \approx 4.7$ GHz, which is close to the relaxation oscillation frequency (ROF) [36] of the 1550 nm VCSEL $f_{RO} = [2\kappa\gamma_e(\mu - 1)]^{1/2}/2\pi = 4.8$ GHz. A single dot in the phase portraits can be seen for this RP state. When the feedback delay time τ is increased to 2.2 ns, the 1550 nm VCSEL enters QP state as shown in Fig. 4(b). The pulsing intensity is modulated and a slowly varying envelope can be observed from the time series. The quasiperiodicity is confirmed from the power spectrum and the phase portraits as well, where different orders of beating and a clear ring are observed. With the increase of the feedback delay time τ, the quasiperiodicity starts to disappear. Finally the 1550 nm VCSEL enters into CP state when τ is 3.1 ns, as shown in Fig. 4(c), where the noise-like intensity fluctuations in the time series and the randomly distributed dots in the phase portrait can be seen. Meantime, the spectrum of the peak series shows a broad band compared with those of the other pulsing states.

According to the previous analysis, to further study, the experimental setup which is shown in Fig. 5 is used to study the nonlinear dynamics of a 1550 nm VCSEL subject to POEF.

3. Experimental Results

The schematic diagram of our experimental setup is shown in Fig. 5. A 1550 nm VCSEL is used in this experiment. The laser is driven by an ultra-low-noise and high-accuracy current source (ILX-Lightwave LDC-3724B), by which the laser temperature can also be controlled. The output from the laser is divided into two parts after passing through an optical isolator (ISO, isolation > 55 dB) and a beam splitter (BS). One is converted to an electrical current and then fed back to the laser to form a delayed positive feedback loop composed of a variable attenuator (VA), an optical delay line (ODL), a photoelectronic detector and an electronic amplifier. The other is collected and simultaneously observed optically and electronically using an optical spectrum analyzer (OSA, Anritsu MS9740A) and an electronic detected system composed of a PD (New Focus 1544-B), a digital oscilloscope (OSC, Agilent DSO91204A), and a radio-frequency (RF) spectrum analyzer (ESA, Agilent N9010A). The output of the laser is monitored and analyzed by the electronic detected system and the OSA.

Fig. 6(a) plots the experimentally measured P–I curve of the free-running 1550 nm VCSEL, showing a threshold current of $I_{th} = 2.1$ mA. Fig. 6(b) shows the optical spectrum of the VCSEL biased at 5.3 mA. The two modes correspond to the two orthogonal polarizations of the fundamental transverse mode of the laser and they are separated by approximately 0.3 nm (38 GHz). In this study, the polarization of the main lasing (about at -11 dBm) and the subsidiary attenuated mode (about at -54 dBm) are referred to as parallel (y) and orthogonal (x) polarizations, respectively.

The controllable parameters of this POEF system are the bias current, the feedback strength, and the feedback delay time. By adjusting these parameters, the system can be operated in different dynamic states. In the experiment, the laser temperature is stabilized at 22.5 °C. The

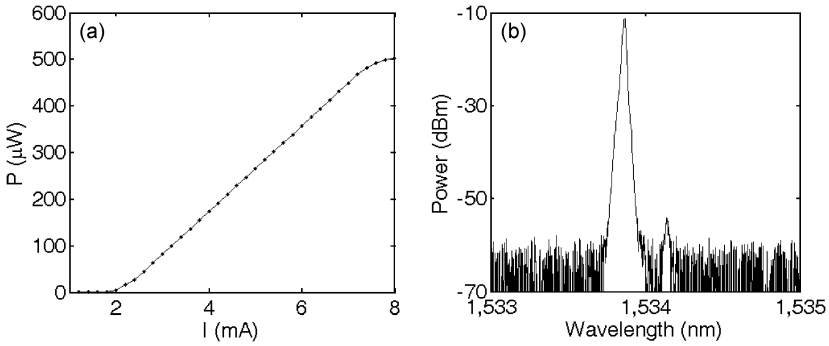

Fig. 6. Experimentally measured (a) P–I curve and (b) optical spectrum of a free-running 1550 nm VCSEL biased at 5.3 mA.

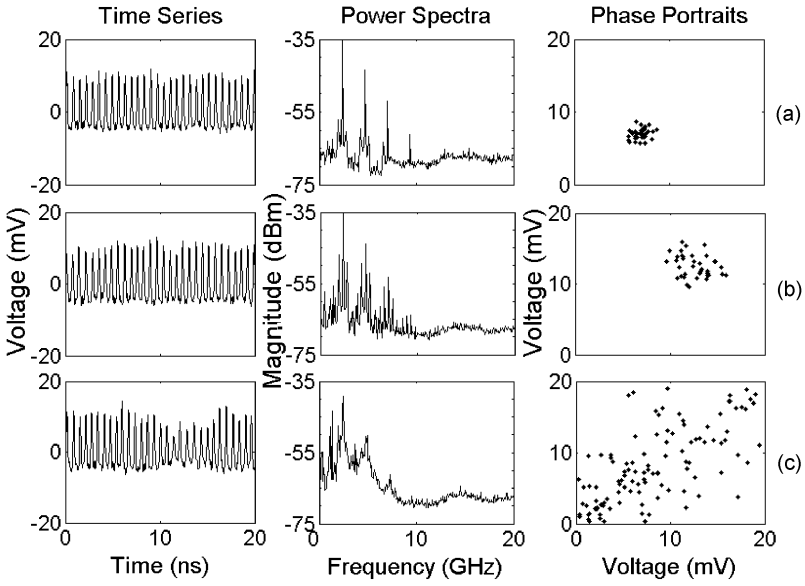

Fig. 7. Experimentally measured time series, power spectra, and phase portraits of different states. (a) RP, (b) QP, and (c) CP states, where the feedback delay time are 210 ps, 280 ps, and 320 ps, respectively.

feedback strength, defined as the ratio of the input optical power of PD in the feedback loop to the solitary VCSEL output power, is fixed at 0.205, and the bias current is fixed at 5.2 mA throughout this experiment. By varying the feedback delay time τ from 210 ps to 320 ps, sequential pulsing states including the RP, QP, and CP states are observed. Fig. 7(a)–(c) shows the time series, the power spectra, and the phase portraits of the state.

For $\tau = 210$ ps, as shown in Fig. 7(a), the output of the POEF system is a RP state, where the time series shows a series of constant intensity pulses. The corresponding power spectra has only one fundamental pulsing frequency at 2.35 GHz. Meanwhile, a dense dot can be seen in the phase portrait. By increasing the feedback delay time τ to 280 ps, as shown in Fig. 7(b), the laser enters a QP state, the pulsing intensity is modulated and a slowly varying envelope can be observed from the time series. Two or above incommensurate frequencies exist in the power spectra, and the phase portrait begins to diffuse. The CP state shown in Fig. 7(c) is then found as τ is increased to 320 ps, where the random intensity pulse can be seen in time series, and the power spectrum is continuous although some sharp peaks remain. Meantime, the phase portrait spreads out over a wide range. Comparing Fig. 7 with Fig. 4, there are some small discrepancies between the theoretical and experimental results. The reason for the

discrepancy is that the parameters of VCSEL used in experiment are different to the parameters of VCSEL used in theoretical analysis. In theoretical analysis, the rate equation model for VCSEL with POEF is based on the SFM. However, it is very difficult that the parameters of VCSEL used in theoretical analysis are entirely agreement with the parameters of VCSEL used in experiment. Although there are some small discrepancies in theoretical and experimental results, in Figs. 4 and 7, the basic dynamic states including the RP, QP, and CP states and the quasiperiodic route to chaos are similar.

4. Conclusion

In this paper, the nonlinear dynamical characteristics of a 1550 nm VCSEL with delayed POEF are studied both numerically and experimentally. The well-established SFM has been extended and generalized to simulate VCSELs subject to OEF by introducing an additional delayed term in the current. Combining the time series, power spectra and phase portraits, it is numerically and experimentally observed that the 1550 nm VCSEL with POEF follows a quasiperiodic scenario to chaos. Although, theoretical and experimental results have some small discrepancies, theory and experiments on the dynamical states of the POEF system under different feedback delay times and the route to chaos are in good agreement.

References

[1] F. Koyama, "Recent advances of VCSEL photonics," *J. Lightw. Technol.*, vol. 24, no. 12, pp. 4502–4513, Dec. 2006.
[2] K. Iga, "Surface-emitting laser—Its birth and generation of new optoelectronics field," *IEEE J. Sel. Topics Quantum Electron.*, vol. 6, no. 6, pp. 1201–1215, Nov./Dec. 2000.
[3] K. Panajotov *et al.*, "Data transparent reconfigurable optical interconnections using polarization switching in VCSEL's induced by optical injection," *IEEE Photon. Technol. Lett.*, vol. 11, no. 8, pp. 985–987, Aug. 1999.
[4] J. Sakaguchi, T. Katayama, and H. Kawaguchi, "All-optical memory operation of 980-nm polarization bistable VCSEL for 20-Gb/s PRBS RZ and 40-Gb/s NRZ data signals," *Opt. Exp.*, vol. 18, no. 12, pp. 12 362–12 370, Jun. 2010.
[5] J. M. Liu, Z. M. Wu, and G. Q. Xia, "Dual-channel chaos synchronization and communication based on unidirectionally coupled VCSELs with polarization-rotated optical feedback and polarization-rotated optical injection," *Opt. Exp.*, vol. 17, no. 15, pp. 12 619–12 626, Jul. 2009.
[6] Z. G. Pan *et al.*, "Optical injection induced polarization bistability in vertical-cavity surface-emitting lasers," *Appl. Phys. Lett.*, vol. 63, no. 22, pp. 2999–3001, Nov. 1993.
[7] C. Masoller and M. S. Torre, "Influence of optical feedback on the polarization switching of vertical-cavity surface-emitting lasers," *IEEE J. Quantum Electron.*, vol. 41, no. 4, pp. 483–489, Apr. 2005.
[8] I. Gatare, M. Sciamanna, J. Buesa, H. Thienpont, and K. Panajotov, "Nonlinear dynamics accompanying polarisation switching in vertical-cavity surface-emitting lasers with orthogonal optical injection," *Appl. Phys. Lett.*, vol. 88, no. 10, Mar. 2006, Art. ID. 101106.
[9] Y. Hong, R. Ju, P. S. Spencer, and K. A. Shore, "Investigation of polarization bistability in vertical-cavity surface-emitting lasers subjected to optical feedback," *IEEE J. Quantum Electron.*, vol. 41, no. 5, pp. 619–624, May 2005.
[10] K. H. Jeong *et al.*, "Optical injection-induced polarisation switching dynamics in 1.5 μm wavelength single-mode vertical-cavity surface-emitting lasers," *IEEE Photon. Technol. Lett.*, vol. 20, no. 10, pp. 779–781, May 2008.
[11] M. S. Torre *et al.*, "Polarization switching in long-wavelength VCSELs subject to orthogonal optical injection," *IEEE J. Quantum Electron.*, vol. 47, no. 1, pp. 92–99, Jan. 2011.
[12] A. Hurtado, I. D. Henning, and M. J. Adams, "Different forms of wavelength polarisation switching and bistability in a 1.55 μm vertical cavity surface emitting laser under orthogonally polarised optical injection," *Opt. Lett.*, vol. 34, no. 3, pp. 365–367, Oct. 2009.
[13] P. S. Spencer, C. R. Mirasso, and K. A. Shore, "Effect of strong optical feedback on vertical cavity surface emitting lasers," *IEEE Photon. Technol. Lett.*, vol. 10, no. 2, pp. 191–193, Feb. 1998.
[14] C.-H. Hang, L. Chrostowski, and C. J. Chang-Hasnain, "Injection locking of VCSELs," *IEEE J. Select. Topics Quantum Electron.*, vol. 9, no. 5, pp. 1386–1393, Sep. 2003.
[15] A. Hurtado, D. Labukhin, I. D. Henning, and M. J. Adams, "Injection locking bandwidth in 1550 nm VCSELs subject to parallel and orthogonal optical injection," *IEEE J. Sel. Topics Quantum Electron.*, vol. 15, no. 3, pp. 585–593, May 2009.
[16] M. Sciamanna *et al.*, "Optical feedback induces polarization mode hopping in vertical-cavity surface-emitting lasers," *Opt. Lett.*, vol. 28, pp. 1543–1545, Sep. 2003.
[17] A. A. Qader, Y. Hong, and K. A. Shore, "Circularly polarized optical feedback effects on the polarization of VCSEL emission," *IEEE Photon. Technol. Lett.*, vol. 24, no. 14, pp. 1200–1202, Jul. 2012.
[18] J. Law and G. Agrawal, "Effects of optical feedback on static and dynamic characteristics of vertical cavity surface emitting lasers," *IEEE J. Sel. Topics Quantum Electron.*, vol. 3, no. 2, pp. 353–358, Apr. 1997.
[19] A. Valle, M. Gomez-Molina, and L. Pesquera, "Polarization bistability in 1550 nm wavelength single-mode vertical-cavity surface-emitting lasers subject to orthogonal optical injection," *IEEE J. Sel. Topics Quantum Electron.*, vol. 14, no. 3, pp. 895–902, May/Jun. 2008.

[20] S. F. Yu, "Nonlinear dynamics of vertical-cavity surface-emitting lasers," *IEEE J. Quantum Electron.*, vol. 35, no. 3, pp. 332–341, Mar. 1999.
[21] J. Buesa, I. Gatare, K. Panajotov, H. Thienpont, and M. Sciamanna, "Mapping of the dynamics induced by orthogonal optical injection in vertical-cavity surface-emitting laser," *IEEE J. Quantum Electron.*, vol. 42, no. 2, pp. 198–207, Feb. 2006.
[22] A. Valle, I. Gatare, K. Panajotov, and M. Sciamanna, "Transverse mode switching and locking in vertical-cavity surface-emitting lasers subject to orthogonal optical injection," *IEEE J. Quantum Electron.*, vol. 43, no. 4, pp. 322–333, Apr. 2007.
[23] M. S. Torre, C. Masoller, and K. A. Shore, "Numerical study of optical injection dynamics of vertical-cavity surface-emitting lasers," *IEEE J. Quantum Electron.*, vol. 40, no. 1, pp. 25–30, Jan. 2004.
[24] A. Hurtado, A. Quirce, A. Valle, L. Pesquera, and M. J. Adams, "Nonlinear dynamics induced by parallel and orthogonal optical injection in 1550 nm vertical-cavity surface-emitting lasers (VCSELs)," *Opt. Exp.*, vol. 18, no. 9, pp. 9423–9428, Apr. 2010.
[25] P. Perez, A. Quirce, L. Pesquera, and A. Valle, "Polarization-resolved nonlinear dynamics induced by orthogonal optical injection in long-wavelength VCSELs," *IEEE J. Quantum Electron.*, vol. 17, no. 5, pp. 1228–1235, Sep. 2011.
[26] R. Al-Seyab *et al.*, "Dynamics of polarization optical injection in 1550 nm VCSELs: Theory and experiments," *IEEE J. Sel. Topics Quantum Electron.*, vol. 17, no. 5, pp. 1242–1249, Sep./Oct. 2011.
[27] K. H. Kim, S. H. Lee, and V. M. Deshmukh, "Dynamics of 1.55 μm wavelength single-mode vertical-cavity surface-emitting laser output under external optical injection," *Adv. Opt. Technol.*, vol. 2012, May 2012, Art. ID. 247070.
[28] F. Y. Lin and J. M. Liu, "Nonlinear dynamics of a semiconductor laser with delayed negative optoelectronic feedback," *IEEE J. Quantum Electron.*, vol. 39, no. 4, pp. 562–568, Apr. 2003.
[29] F. Y. Lin and J. M. Liu, "Harmonic frequency locking in a semiconductor laser with delayed negative optoelectronic feedback," *App. Phys. Lett.*, vol. 81, no. 17, pp. 3128–3130, Oct. 2002.
[30] S. Tang and J. M. Liu, "Chaotic pulsing and quasi-periodic route to chaos in a semiconductor laser with delayed opto-electronic feedback," *IEEE J. Quantum Electron.*, vol. 37, no. 3, pp. 329–336, Mar. 2001.
[31] W. L. Zhang *et al.*, "Theoretical study on polarization dynamics of VCSELs with negative optoelectronic feedback," *Appl. Opt.*, vol. 46, no. 29, pp. 7262–7266, Oct. 2007.
[32] J. F. Liao and J. Q. Sun, "Polarization dynamics and chaotic synchronization in unidirectionally coupled VCSELs subjected to optoelectronic feedback," *Opt. Commun.*, vol. 295, pp. 188–196, May 2013.
[33] Y. Y. Xie *et al.*, "Nonlinear dynamics of 1550 nm VCSELs subject to positive optoelectronic feedback," *IEEE Photon. Technol. Lett.*, vol. 25, no. 16, pp. 1605–1608, Apr. 2013.
[34] J. Martin-Regalado, F. Prati, M. San Miguel, and N. B. Abraham, "Polarization properties of vertical-cavity surface-emitting lasers," *IEEE J. Quantum Electron.*, vol. 33, no. 5, pp. 765–783, May 1997.
[35] M. San Miguel, Q. Feng, and J. V. Moloney, "Light-polarization dynamics in surface-emitting semiconductor lasers," *Phys. Rev. A*, vol. 52, no. 2, pp. 1728–1739, Aug. 1995.
[36] N. Khan, K. Schires, A. Hurtado, I. D. Henning, and M. J. Adams, "Measurement of temperature-dependent relaxation oscillation frequency and linewidth enhancement factor of a 1550 nm VCSEL," *IEEE J. Quantum Electron.*, vol. 49, no. 11, pp. 990–996, Sep. 2013.